International Journal of Thin Films Science and Technology

http://dx.doi.org/10.18576/ijtfst//130106

Heat and Mass transfer effect in Stagnation point flow of MHD Jeffery Nanofluid Flow over Porous Stretching sheet with Thermal Radiation

Kapil Kumar [1], Bhupander singh [1], Pravendra Kumar [1,], Kottakkaran Sooppy Nisar [2], Abdel-Haleem Abdel-Aty [3], Shawkat Alkhazaleh [4] and Mahmoud Abdel-Aty [5,6,7]*

[1] Department of Mathematics, Meerut College, Meerut-250003, Uttar Pradesh, India
[2] Department of Mathematics, College of Science and Humanities in Alkharj, Prince Sattam Bin Abdulaziz University, Alkharj 11942, Saudi Arabia
[3] Department of Physics, College of Sciences, University of Bisha, Bisha 61922, Saudi Arabia
[4] Department of Mathematics, Faculty of Sciences and Information Technology, Jadara University, Irbid, Jordan
[5] Department of Computer Science and Information Engineering, Chung Hua University, 707, WuFu Rd., Hsinchu, Taiwan 30012, R.O.C.
[6] Deanship of Graduate Studies and Research, Ahlia University, P.O. Box 10878 Manama, Kingdom of Bahrain
[7] Mathematics Department, Faculty of Science, Sohag University, P.O. Box 82524, Sohag, Egypt

Received: 4 Aug. 2023, Revised: 18 Dec. 2023, Accepted: 22 Dec. 2023
Published online: 1 Jan. 2024

Abstract: The current perusal is focused on the investigation of stagnation point flow of Magnetohydrodynamics (MHD) nanofluids across a porous stretching sheet utilizing Jeffery model. Additionally, the impact of thermal radiation has been considered. Through the selection of appropriate similarity transformations, the partial differential equations have been converted into non-linear ordinary differential equations and subsequently extricated numerically utilizing BVP4c technique in MATLAB software. The effects of significant variables like as $\lambda_2, M, K, r, \beta, Pr, Nr, N_b, N_t$ and Le have been thoroughly discussed and illustrated through graphical representation..

Keywords: Nanofluid, Jeffery fluid, Hydromagnetic, stagnation point flow, thermal radiation, stretching sheet.

1 Introduction

At a point of stagnation, the flow field's velocity with respect to the body and the fluid's particles is zero. At the flow field's object surfaces, where the fluid is dragged to the rest by the object, stagnation points exist. The Bernoulli equation states that, static pressure is at its highest level at stagnation points since it is at its maximum value when the velocity is at rest. The idea of two-dimensional stagnation flows was initially put out by Hiemenz [1]. The axisymmetric stagnation point flow represents a fundamental and highly stable system that arises in situations involving flow pace in two similar segments and skin-contact with mass and heat exchange in the vicinity of the stagnation region. In addition, the utilization of push bearings and spiral diffusers, the reduction of drag at the corner's edge, transpiration cooling, and thermal oil recovery are all basic applications of stagnation point. Pop et al. [2] expound upon the influence of radiation on the flow at the stagnation point of a stretched sheet. Their study showcases the formation of a boundary layer, elucidates the impact of temperature, radiation, and velocity on its thickness, and establishes a negative correlation between Prandtl number and boundary layer thickness. Dutta et al. [3] examine the temperature distribution across a stretching sheet. The authors illustrate that the sheet experiences a uniform heat flux and the velocity of the sheet is directly proportionate to the length of the slit. Furthermore, it is shown that rise in the Prandtl number causes a temperature reduces at a specific place. The phenomenon of steady stagnation-point flow across an elastic surface was first examined by Chiam [4], wherein the equivalent magnitudes of free stream and stretching velocities were considered. Mahapatra and Gupta [5] conducted an investigation on the flow issue by carefully selecting diverse stretching and free stream velocities. Through this meticulous

* Corresponding author e-mail: pkumar0106@gmail.com

examination, they were able to confirm the existence of boundary layers. Ramana et al. [6] conducted an explication of the steady magnetohydrodynamic stagnation point fluid flow of a Casson fluid through a stretched sheet with heat source and chemical reaction of first-order, incorporating multiple slip boundary conditions. Their findings indicated that increased heat source and chemical reaction parameters resulted in a decrease in chemical reaction and temperature profile. Nandi et al. [7] utilized statistical and numerical perspective to investigate the issue of stagnation point flow of MHD methanol-based nanofluid through convectively heated stretched sheet, accounting for influence of thermal radiation and heat generation via a porous media. Asogva et al. [8] discovered radiative characteristics of electromagnetohydrodynamic across an induced stagnation point flow through a stretched surface utilizing Casson nanofluid, considering effects of chemical reaction and thermal radiation. Reddy et al. [9] explored numerical results of the magnetohydrodynamictwo-dimensional stagnation point flow of an incompressible nanofluid flow across a stretchable cylinder, accounting for effects of convective boundary conditions and radiation. Their findings indicated that an enhancement in Biot number and thermal radiation parameter resulted in upsurge in profile of temperature and concentration boundary layer of nanoparticles, while rise in the Brownian motion and thermophoresis parameter values resulted in a scarcity in rate of heat transfer. Khan et al. [10] examined the MHD stagnation point flow ofJeffery nanofluid for stretched surface accompanied by Cattaneo-Christov mass and heat fluxes, demonstrating the impact of sundry variables on velocity, thermal boundary layer, and profile of concentration. Numerous studies [11,12,13,14,15,16,17,18,19,20] examined various aspects of MHD stagnation point flow.

The perusal of nanofluids has been a subject of extensive research because of the significant increase in thermal conductance of liquids throughout heat transmission with the presence of nanomolecules [21,22]. A liquid containing nanomolecules between 1-100 nm is indicated as a nano liquid. Nanofluids, a unique class of composite materials, suspend solid particles as small as a nanometer in typical heat transfer fluids like as water,toluene,motor oil and ethylene glycol. The main characteristic of nanofluids is their heat conductivity is superior to that of base fluids.One of the most noteworthy occurrencesassociated with nanofluids is rise in thermal conductivity, surpassing the limiting heat transfer capability of contemporary basic fluids. The aforementioned fluids are used in distinctive mannersto enhance heat transmission and thermal conductivity. The term ”nanofluid” was invented by Choi [23] while investigating novel coolants and cooling techniques. Research by Estman et al. [24] indicates thata dispersion of copper nanoparticles within ethylene glycol exhibits a significantly elevated effective thermal conductivity compared to ethylene glycol containing the samilar volume percent of scattered oxide nanometer-sized particles. Bachok et al. [25] examined and provide a solution by killer box method for the issue at hand pertains to the steady boundary layernanofluid flow of over a semi-infinite flat plate in motion. They demonstrate the presence of two distinct solutions when plate and the free stream exhibit opposing motiondirections.Priyadharshinni et al. [26] conducted an investigated the magnetohydrodynamics (MHD) of an incompressible boundary layer nanofluid flow that occurs across a porous stretchable sheet oriented vertically. Their study utilized Bougirno’s design while taking into account the convective states. The implementation of themodel of nanofluid was achieved through utilization of thermophoresis and Brownian motion effects. In various thermodynamic processes and the optimization of thermal processing, the nanofluid flow over a stretchable surface that is implanted vertically across a porous medium explored by Hussain and sheremet [27].Hosseinzadeh et al. [28] conducted an inquiry into the behavior of a non-Newtonian nanofluid exhibiting viscoelastic properties in second grade, as it flowed through a curve stretching surface under the influence of magnetohydrodynamics in a two-dimensional mode.The authors have provided evidence that the force of drag on a surface is dependent on the nature of non-Newtonian fluids, with an increasing correlation observed. Additionally, concentration and velocity of the viscous fluid are observed to decrease more rapidly in comparison to viscoelastic fluids. The role that a nanoparticle’s increased radius hasthe impact of the magnetic field on energy flow is also considered over concentration panels and mass flux via temperature distribution analysed by Manzoor et al. [29]. Rehmanet al. [30] conducted research on micropolar nanofluid flow with MHD effects, considering thermal radiation and buoyancy parameter across a stretched and shrinking sheet and problemnumerically solved using RK method with shooting technique. Numerous researchers have looked at the topic of nanofluid flow recently [31,32,33,34,35,36,37] with an understanding of all such inquiries.

The impact of thermal radiation on mass and heat transfer across a stretched surface is of great significance in the realm of physics and engineering, owing to its wide-ranging applicability encompassing nuclear power plants, fossil fuel combustion, gas turbines, liquid metal fluids, photoionization, plasma wind tunnels, geophysics, and various propulsion devices such as missiles, aircraft, spacecraft, and satellites [38]. The influence ofviscous dissipation and thermal radiation on MHD nanofluid flow across porous stretched surface is examined by Muntazir et al. [39].They discovered that heat transfer rate exhibited by copper nanoparticles exceeds that of aluminium oxide nanoparticles. Deniel et al. [40] have provided a comprehensive discussion on electrical magnetohydrodynamic natural convection nanofluid flow across stretched sheet, considering impacts of chemical reaction and thermal radiation. It was discovered that through manipulation of thermal radiation parameter, the fluid’s temperature exhibited an observable increase. Mass and heat transfer of nanofluid with thermal radiation together with stretchable sheet in existence of convective heating and slip velocity phenomenon investigated by Alrehili [41]. Using a quadratic stretching plate and nonlinear thermal radiation, numerical simulation is used to discuss the melting heat transfer of nanofluids analysed by Muhammad et al. [42]. They found that the mechanical properties of the working liquid as well as its thermal efficiency may be successfully improved by carbon nanotubes. Some related works are presented in references [43,44,45].

Jeffrey's fluid model, one of numerous non-Newtonian models suggested, is notable because model of Newtonian fluid can be inferred from this as a special case by accepting $\lambda_1 = 0$. Additionally, it is hypothesised that during blood circulation in a living body, physiological fluids like blood exhibit Newtonian and non-Newtonian behaviours [46,47,48,49]. The Jeffrey's model has shown to be highly successful, as have a number of other rheological models developed. Some interesting studies [50,51,52] employing Jeffery fluid model with the influence of magnetohydrodynamic (MHD).

2 Mathematical formulation

In the current mathematical model, we consider a laminar,steady, two-dimensional magnetohydrodynamic flow of an incompressible, viscous fluid that occurs close to a stagnation point on surface in porous medium. This surface is saturated by a Jeffery nanofluid and coincides with the plane y=0. Furthermore, the flow takes place at $y \geq 0$ (see fig. A). The measurement of y is performed in a direction that is perpendicular to the stretching sheet. Here, we take the surface's stretching into consideration with the velocity $U_w(x) = bx$ linearly, whereas b is a constant with positive value and x is quantified along the sheet that is being stretched. The temperature of the surface and concentration of the fluid at the surface of stretching sheet have constant values T_w and C_w, respectively, while the temperature and concentration in the surrounding environment, at a distance away from the surface, are denoted as T_∞ and C_∞, correspondingly.

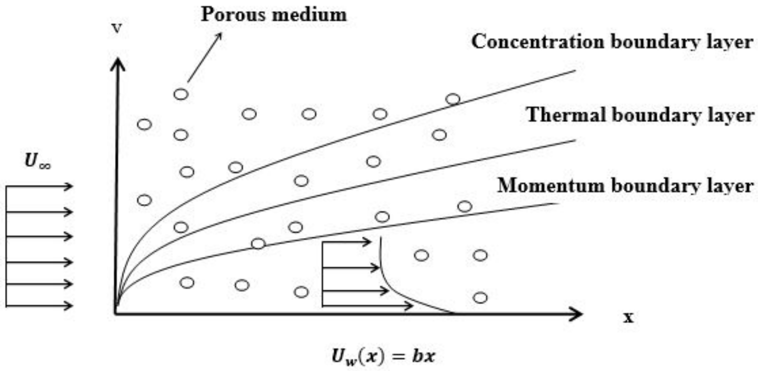

Fig. A: Geometry of the problem

Under the aforementioned fundamental postulations, the governing equation of conservation of mass, momentum, energyand concentration of nanoparticlefor steady flow with the influence of thermal radiation across a porous stretching sheet are as follows:

$$\frac{\partial u}{\partial x} + \frac{\partial v}{\partial y} = 0 \tag{1}$$

$$u\frac{\partial u}{\partial x} + v\frac{\partial u}{\partial y} = U_\infty \frac{\partial U_\infty}{\partial x} + \nu \frac{\partial^2 u}{\partial y^2} + \frac{\nu}{1+\lambda_2}\left[\frac{\partial^2 u}{\partial y^2} + \lambda_1\left(u\frac{\partial^3 u}{\partial x \partial y^2} + v\frac{\partial^3 u}{\partial y^3} - \frac{\partial u}{\partial x}\frac{\partial^2 u}{\partial y^2} + \frac{\partial u}{\partial y}\frac{\partial^2 u}{\partial x \partial y}\right)\right] - \nu\frac{(u-U_\infty)}{\kappa_1} - \frac{\sigma B_0^2}{\rho}(u-U_\infty) \tag{2}$$

$$u\frac{\partial T}{\partial x} + v\frac{\partial T}{\partial y} = \alpha\frac{\partial^2 T}{\partial y^2} + \frac{(\rho c_p)_p}{(\rho c_p)_f}\left[D_B\frac{\partial T}{\partial y}\frac{\partial C}{\partial y} + \frac{D_T}{T_\infty}\left(\frac{\partial T}{\partial y}\right)^2\right] - \frac{1}{(\rho C_p)}\frac{\partial q_r}{\partial y} \tag{3}$$

$$u\frac{\partial C}{\partial x} + v\frac{\partial C}{\partial y} = D_B\left(\frac{\partial^2 C}{\partial y^2}\right) + \frac{D_T}{T_\infty}\left(\frac{\partial^2 T}{\partial y^2}\right) \tag{4}$$

The problem's boundary conditions are precisely delineated as follows:

$$u = u_w = bx, \quad v = 0, \quad T = T_w, \quad C = C_w, \quad \text{at} \quad y = 0 \tag{5}$$

$$u = u_e \to 0, \quad T = T_\infty, \quad C = C_\infty \quad \text{as} \quad y \to \infty \tag{6}$$

Where u and v signify the velocity components of the Jeffery nanofluid inx and ydirections, respectively, $U_\infty = ax$ signifies straining velocity of the stagnation point flow, wherein $a > 0$ denotes straining constant.
In the equation governing the boundary layer of energy (3), the radiative heat flux q_r is approximated utilizing Rosseland approximation [53] for thermal radiation, as follows:

$$q_r = -\frac{4\sigma^*}{3k^*}\frac{\partial T^4}{\partial y} \tag{7}$$

Whereas σ^* denotes the Stephan Boltzmann constant, k^* signifies Rosseland mean spectral absorption coefficient.
By employing a Taylor series expansion centered at the ambient temperature T_∞, it is possible to discern that the term T^4 can be regarded as a linear relationship with temperature. This can be achieved by neglecting higher order terms in the approximation process.

$$T^4 \cong 4{T_\infty}^3 T - 3{T_\infty}^4 \tag{8}$$

Using Equations(7) and (8), we obtain

$$\frac{\partial q_r}{\partial y} = -\frac{16\sigma^* {T_\infty}^3}{3k^*}\frac{\partial^2 T}{\partial y^2} \tag{9}$$

To achieve a reduction of the governing nonlinear partial differential equations, it is necessary to employ a set of non-dimensional similarity transformations. These transformations will lead to the formulation of non-dimensional ordinary differential equations.

$$\begin{cases} \eta = \sqrt{\frac{b}{\nu}}y, \quad \psi = \sqrt{b\nu}f(\eta), \quad u = bxf'(\eta), v = -\sqrt{b\nu}f'(\eta) \\ \theta(\eta) = \frac{(T - T_\infty)}{(T_w - T_\infty)}, \quad \phi(\eta) = \frac{c - c_\infty}{c_w - c_\infty} \end{cases} \tag{10}$$

Where $b > 0$,the stream function ψ is precisely defined as $u = \partial\psi/\partial y$ and $v = -\partial\psi/\partial y$. Eq. (1) is fulfils in identical manner as well as equations (2) - (4) together with boundary conditions (5) - (6) are converted into the following ordinary differential equations by utilizing dimensionless variables.

$$f'''(\eta) + \beta\left[\left(f''(\eta)\right)^2 - f(\eta)f^{iv}(\eta)\right] + (1+\lambda_2)\left[f'''(\eta) + f(\eta)f''(\eta) + r^2 - \left(f'(\eta)\right)^2 - (M+K)\left(r - f'(\eta)\right)\right] = 0 \tag{11}$$

$$(1+Nr)\theta''(\eta) + Pr\left[f(\eta)\phi'(\eta) + N_b\theta'(\eta)\phi'(\eta) + N_t\left(\theta'(\eta)\right)^2\right] = 0 \tag{12}$$

$$\phi''(\eta) + LePrf(\eta)\phi'(\eta) + \frac{N_t}{N_b}\theta''(\eta) = 0 \tag{13}$$

Using similarity variables into the boundary conditions (5) - (6), we get

$$\begin{cases} f(0) = 0, \quad f'(0) = 1, \quad \theta(0) = 1, \quad \phi(0) = 1 \\ f'(\eta) \to r, \quad \theta(\eta) \to 0, \quad \phi(\eta) \to 0 \quad \text{as} \quad \eta \to \infty \end{cases} \tag{14}$$

Primes are utilized to indicate the process of differentiation with regard to η.
The specified parameters are characterized as:

$$M = \frac{\sigma {B_0}^2}{b\rho}, \quad K = \frac{\nu}{bk_1}, \quad r = \frac{a}{b}, \quad \beta = \lambda_1 b, \quad \Pr = \frac{(\rho C_p)\nu}{k_f}, \quad Nr = \frac{16}{3}\frac{\sigma^*}{k^* k_f}T_\infty^3$$
$$N_b = \frac{\tau D_B}{\nu}(C_w - C_\infty), \quad N_t = \frac{\tau D_T}{T_\infty \nu}(T_w - T_\infty), \quad Le = \frac{\alpha_D}{D_B}$$

Where M denote the magnetic parameter, K stands for the porous parameter, r is the stagnation parameter, β is the Deborah number, Pr denote Prandtl number, Nr be the radiation parameter, N_b is Brownian motion parameter, N_t shows

thermophoresis parameter and Le is Lewis number.
The skin friction coefficient, heat transfer rate, and Sherwood number are the essential physical quantities of concern. These quantities are formulated as such.

$$C_f = \frac{\tau_w}{\frac{\rho}{2}{u_w}^2}, \quad Nu_x = \frac{xq_w}{k_f\,(T_w - T_\infty)}, \quad Sh_x = \frac{xq_m}{D_B\,(C_w - C_\infty)} \tag{15}$$

Where τ_w denote wall shear stress, surface heat flux is q_w and q_m shows mass flux which can be determined as

$$\begin{aligned} \tau_w &= \frac{\mu}{1+\lambda_2}\left[\frac{\partial u}{\partial y} + \lambda_1\left(u\frac{\partial^2 u}{\partial x \partial y} + u\frac{\partial^2 v}{\partial x^2} + v\frac{\partial^2 u}{\partial y^2}\right)\right]\bigg|_{y=0}, \\ q_w &= -\left(k_f + \frac{16}{3}\frac{\sigma^*}{k^*}T_\infty^3\right)\frac{\partial T}{\partial y}\bigg|_{y=0}, \\ q_m &= -D_B\left(\frac{\partial c}{\partial y}\right)\bigg|_{y=0} \end{aligned} \tag{16}$$

Using similarity variables, we obtain

$$\begin{aligned} \frac{1}{2}\sqrt{Re_x}C_f &= \frac{1}{1+\lambda_2}\left[f''(0) + \beta\left(f'(0)f''(0) - f(0)f'''(0)\right)\right], \\ \frac{Nu_x}{\sqrt{Re_x}} &= -(1+Nr)\theta'(0), \frac{Sh_x}{\sqrt{Re_x}} = -\phi'(0) \end{aligned} \tag{17}$$

3 Solution Method

The MATLAB function bvp4c has been employed to implement the collocation strategy for the purpose of addressing boundary value problems.The bvp4c algorithm is used in this analysis to compute the computational outcomes of the equations (11), (12) and (13) with boundary condition (14). The differential equations (11), (12), and (13) must be converted into first order ODEs in order to implement the bvp4c algorithm.

$$f = y_1, \;\; f' = y_2, \;\; f'' = y_3, \;\; f''' = y_4, \;\; \theta = y_5, \;\; \theta' = y_6, \;\; \phi = y_7, \;\; \phi' = y_8 \tag{18}$$

Equations (11), (12), (13), and (14) become

$$y_1{}' = y_2 \tag{19}$$
$$y_2{}' = y_3 \tag{20}$$
$$y_3{}' = y_4 \tag{21}$$
$$y_4{}' = \frac{1}{y_1}\left[{y_3}^2 + \frac{1}{\beta}\left[(1+\lambda_2)\left\{y_4 + y_1y_3 + r^2 - {y_2}^2 - (M+K)(r - y_2)\right\} + y_4\right]\right] \tag{22}$$
$$y_5{}' = y_6 \tag{23}$$
$$y_6{}' = -\frac{Pr}{(1+Nr)}\left[y_1y_8 + N_by_6y_8 + N_t{y_6}^2\right] \tag{24}$$
$$y_7{}' = y_8 \tag{25}$$
$$y_8{}' = -LePry_1y_8 + \frac{N_tPr}{N_b(1+Nr)}\left[y_1y_8 + N_by_6y_8 + N_t{y_6}^2\right] \tag{26}$$

The boundary condition yields

$$\begin{cases} y_1(0) = 0, \quad y_2(0) = 1, \quad y_5(0) = 1, \quad y_7(0) = 1 \text{ at } \quad \eta \to 0 \\ y_2(\eta) = r, \quad y_5(\eta) = 0, \quad y_7(\eta) = 0 \quad \text{at} \quad \eta \to \infty \end{cases} \tag{27}$$

4 Result and Discussion

To address boundary value problems that involve boundary conditions, the bvp4c function is utilized within the MATLAB software package. Heat and mass transfer in stagnation point flow of steady two-dimensional Jeffery nanofluids across a porous stretched sheet with the effects of magnetohydrodynamics and thermal radiation have been analyzed in this paper. As previously noted, the equations that govern the MHD Jeffery nanofluid flow through a permeable stretched sheet with the influence of thermal radiation (equations (11)-(13)) together with boundary condition equation (14) have been numerically solved via utilization of the bvp4c MATLAB process.After the application of the aforementioned process and subsequent resolution of the problem at hand, the effect of several non-dimensional parameters $\lambda_2, N_t, N_b, Pr, r, M, K, Nr, Le$ and β on velocity, temperature and concentration profiles have been thoroughly examined and discussed. Results for varying valuesof the governing parameters are presented graphically in figures (1)-(13). The numerical computation of local skin fraction coefficient, local heat transfer coefficient and the coefficient of mass transfer are obtained for various parameters and presented in tabular form in Tables 1 and 2 respectively.

Figure 1(a) depicts the impact of porosity parameter on fluid's velocity. On rising the value of porosity parameter, the velocity profile rises. Figure 1(b) illustrates the influence of λ_2 on fluid's velocity. It is notable that the velocity profile undergoes a reduction when the value of λ_2 experiences an increment for the stretching sheet.

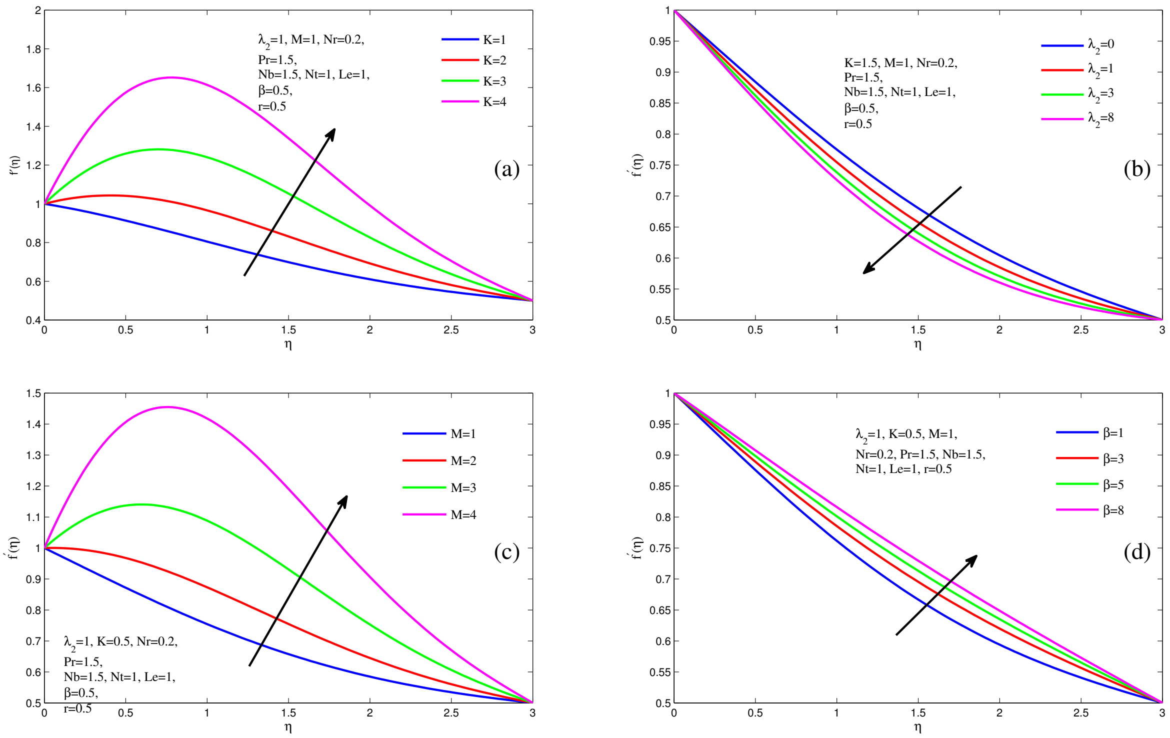

Fig. 1: Influence of the system parameters on non-dimensional velocity profile, where (a) Influence of porosity parameter K, (b) Influence of λ_2, (c) Influence of the magnetic parameter M and (d) Influence of Deborah number β.

Figure 1(c) depicts the change in the velocity of the Jeffery Nanofluid with magnetic parameter M. It should be noticed that when the magnetic parameter M rises, an augmentation in fluid's velocity is discerned.

Figure 1(d) displays variations in velocity profile when considering varying values of the Deborah number β pertaining to Jeffery nanofluid. The velocity of the Jeffery nanofluid is observed to escalate with the augmentation of the Deborah number β, as depicted in Figure 1(d). Change in dimensionless velocity with r is plotted in the figure 2. It is evident that that the velocity profile shows a linearly increasing behavior between $0 < r \leq 1$ whereas the velocity of the Jeffery Nanofluid flow shows a parabolically increasing behavior for $r > 1$.

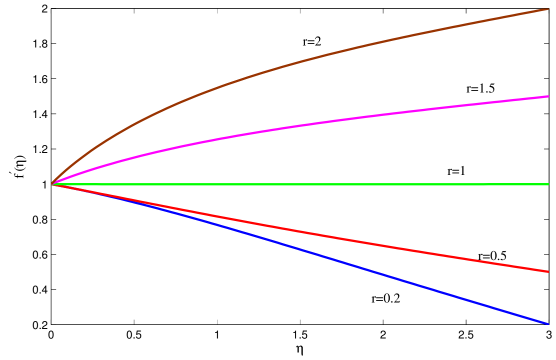

Fig. 2: Influence of stagnation point parameter r on non-dimensional velocity parameter.

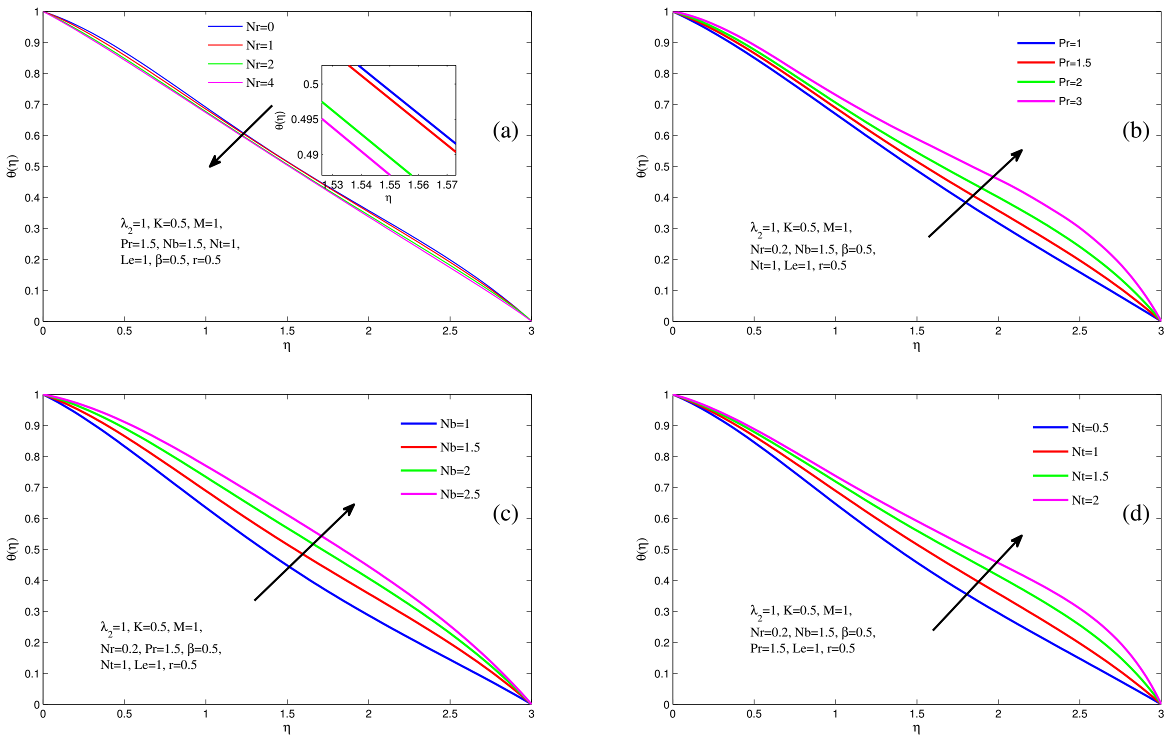

Fig. 3: Influence of the system parameters on non-dimensional temperature profile, where (a) Influence of thermal radiation parameter Nr, (b) Influence of Prandtl Number Pr, (c) Influence of Brownian motion parameter N_b and (d) Influence of thermophoresis parameter N_t.

Variation of dimensionless temperature with thermal radiation parameter is displayed in figure 3(a). It is evident from the depiction provided in figure 3(a) that profile of temperature decreases as value of thermal radiation parameter Nr increases.

Figure 3(b) is depicted to emphasize the effect of Prandtl number Pr on profile of temperature. It is evident from the depiction provided in figure 3(b) that temperature of the Jeffery nanofluid upsurges with the escalating value of Prandtl number Pr.

Figure 3(c) is prepared to illustrate the effect of Brownian motion parameter N_b, exerts upon temperature field for viscous and thermal forces. It shows that the temperature profile experiences an upsurge in behavior upon the increment of Brownian motion parameter N_b.The thermophoresis parameter N_t is emphasized in figure 3(d) to characterize memory properties on temperature distribution. It has been discovered that an increase in the thermophoresis parameter N_t yields a consequential augmentation in temperature profile $\theta(\eta)$.

Figure 4(a) reveals the impact of Le on the distribution of volume fractions of nanoparticles. It is demonstrated that the rising values of Lewis number consequences in decline in the profileof concentration.The figure 4(b) depicts the influence of variation in Pr on the profile of nanoparticle fraction. As the Prandtl number Pr rises, it has been observed that concentration profile experiences a reduction.

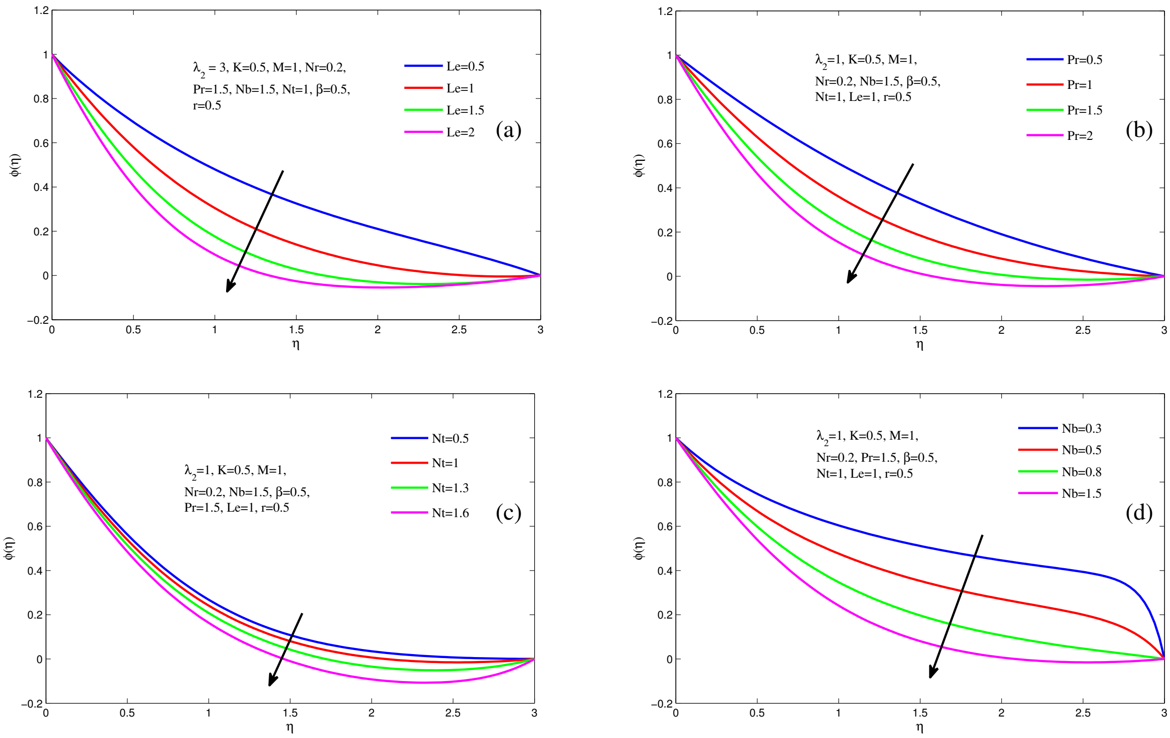

Fig. 4: Influence of the system parameters on non-dimensional concentration profile, where (a) Influence of Lewis number Le, (b) Influence of Prandtl number Pr, (c) Influence of thermophoresis parameter N_t and (d) Influence of Brownian motion parameter N_b.

Figure 4(c) illustrates the change in profile of concentration with respect to the Thermophoresis parameter N_t.It has been discovered that rise in the thermophoresis parameter N_t is associated with a reduction in concentration profile.Figure 4(d) displays variations in concentration curves for different quantities of N_b. It is noted that with rising value of Brownian motion factor N_b, a decrement is observed in nanoparticle fraction of the fluid.

Table 1 portrays the effect of flow parameters, λ_2, K, M, β and r on skin frictioncoefficient. It is observed from Table 1 that, magnitude of skin friction coefficient is augmented with higher values of magnetic parameter, porosity parameter and Deborah number, whereas in increase in stagnation point parameter and λ_2 leads to reduction in the skin friction coefficient.

Table 2 portrays the influences of $\lambda_2, N_t, N_b, Pr, r, M, K, Nr, Le$ and β on temperature gradient and mass transfer coefficient for stretching sheet of Jeffery nanofluid. It demonstrates that coefficient of heat transfer upsurges with an escalation in values of $\lambda_2, K, M, \beta, Nr$ and Le whereas in increases in N_t, N_b, Pr and r leads to decreases in the heat transfer coefficient. The coefficient of mass transfer is enhanced with increased in N_t, N_b, Pr, r and Le whereas decrease with increase in λ_2, K, M, β and Nr.

Table 1: Effect of various parameteron C_f

λ_2	K	M	β	r	$\frac{1}{2}\sqrt{Re_x}C_f$
1	0.6	3	0.5	0.5	0.2430
2	0.6	3	0.5	0.5	0.2235
3	0.6	3	0.5	0.5	0.2004
4	0.6	3	0.5	0.5	0.1797
1	0.5	3	0.5	0.5	0.2138
1	1.0	3	0.5	0.5	0.3734
1	1.5	3	0.5	0.5	0.5703
1	2.0	3	0.5	0.5	0.8096
1	0.6	0.5	0.5	0.5	0.2430
1	0.6	1.0	0.5	0.5	0.4096
1	0.6	1.5	0.5	0.5	0.6147
1	0.6	2.0	0.5	0.5	0.8628
1	0.6	2	0.5	0.5	0.2430
1	0.6	2	1.0	0.5	0.4422
1	0.6	2	1.5	0.5	0.6224
1	0.6	2	2.0	0.5	0.7958
1	0.6	3	0.5	0.2	0.5754
1	0.6	3	0.5	0.3	0.4512
1	0.6	3	0.5	0.4	0.3400
1	0.6	3	0.5	0.6	0.1614

Table 2: Effects of various parameter on Sherwood number and Nusselt number.

λ_2	K	M	Nr	Pr	r	Le	N_b	N_t	β	$-(1+N_r)\theta'(0)$	$-\phi'(0)$
1	0.6	2	0.4	1	0.5	1	0.6	1	0.5	0.5356	0.6117
2	0.6	2	0.4	1	0.5	1	0.6	1	0.5	0.5391	0.6079
3	0.6	2	0.4	1	0.5	1	0.6	1	0.5	0.5416	0.6052
4	0.6	2	0.4	1	0.5	1	0.6	1	0.5	0.5434	0.6032
1	0.5	2	0.4	1	0.5	1	0.6	1	0.5	0.5344	0.6129
1	1.0	2	0.4	1	0.5	1	0.6	1	0.5	0.5409	0.6062
1	1.5	2	0.4	1	0.5	1	0.6	1	0.5	0.5480	0.5987
1	2.0	2	0.4	1	0.5	1	0.6	1	0.5	0.5557	0.5906
1	0.6	3.0	0.4	1	0.5	1	0.6	1	0.5	0.5356	0.6117
1	0.6	3.5	0.4	1	0.5	1	0.6	1	0.5	0.5423	0.6048
1	0.6	4.0	0.4	1	0.5	1	0.6	1	0.5	0.5494	0.5971
1	0.6	4.5	0.4	1	0.5	1	0.6	1	0.5	0.5573	0.5889
1	0.6	2	0.3	1	0.5	1	0.6	1	0.5	0.4705	0.6477
1	0.6	2	0.4	1	0.5	1	0.6	1	0.5	0.5034	0.6283
1	0.6	2	0.6	1	0.5	1	0.6	1	0.5	0.5670	0.5978
1	0.6	2	0.7	1	0.5	1	0.6	1	0.5	0.5981	0.5866
1	0.6	2	0.4	0.8	0.5	1	0.6	1	0.5	0.5450	0.5246
1	0.6	2	0.4	0.9	0.5	1	0.6	1	0.5	0.5404	0.5676
1	0.6	2	0.4	1.1	0.5	1	0.6	1	0.5	0.5307	0.6565
1	0.6	2	0.4	1.3	0.5	1	0.6	1	0.5	0.5208	0.7482
1	0.6	2	0.4	1	0.2	1	0.6	1	0.5	0.5460	0.5999
1	0.6	2	0.4	1	0.3	1	0.6	1	0.5	0.5423	0.6042
1	0.6	2	0.4	1	0.4	1	0.6	1	0.5	0.5386	0.6081
1	0.6	2	0.4	1	0.6	1	0.6	1	0.5	0.5331	0.6146
1	0.6	2	0.4	1	0.5	0.8	0.6	1	0.5	0.5273	0.5407
1	0.6	2	0.4	1	0.5	1.0	0.6	1	0.5	0.5356	0.6117
1	0.6	2	0.4	1	0.5	1.2	0.6	1	0.5	0.5432	0.6931
1	0.6	2	0.4	1	0.5	1.4	0.6	1	0.5	0.5493	0.7839
1	0.6	2	0.4	1	0.5	1	0.6	1	0.5	0.5356	0.6117
1	0.6	2	0.4	1	0.5	1	0.7	1	0.5	0.5331	0.6616
1	0.6	2	0.4	1	0.5	1	0.8	1	0.5	0.5231	0.7121

1	0.6	2	0.4	1	0.5	1	0.9	1	0.5	0.5010	0.7709
1	0.6	2	0.4	1	0.5	1	0.6	0.6	0.5	0.6403	0.5596
1	0.6	2	0.4	1	0.5	1	0.6	0.8	0.5	0.5809	0.5642
1	0.6	2	0.4	1	0.5	1	0.6	1.2	0.5	0.5030	0.6839
1	0.6	2	0.4	1	0.5	1	0.6	1.6	0.5	0.4597	0.7714
1	0.6	3	0.5	1	0.5	1	0.6	1	0.5	0.5356	0.6117
1	0.6	3	0.5	1	0.5	1	0.6	1	1.0	0.5397	0.6073
1	0.6	3	0.5	1	0.5	1	0.6	1	1.5	0.5418	0.6052
1	0.6	3	0.5	1	0.5	1	0.6	1	2.0	0.5430	0.6039

5 Conclusion

This analysis comprehensively elucidates the magnetohydrodynamic stagnation point flow of a steady Jeffery nanofluid in the presence of thermal radiation effects through a porous stretching sheet. On various physical quantities, the impacts of various influencing parameters are investigated. The results are established using the bvp4c software; the following is a compendium of the results:
1- As the value of β, K and M rises, the momentum boundary layer gradually increases away from the sheet.
2- Velocity of the fluid has decreasing behavior for greater values of λ_2.
3- Temperature profile rises when Prandtl number, Brownian motion parameter and thermophoresis parameter enhances.
4- With an enhance in Le, Pr, N_t, and N_b, the concentration boundary layer thickness diminishes.
5- The Nusselt number is reducible with the elevation of λ_2, K, M, Nr, Le and β.
6- As the value of K, M and β rise, so does the coefficient of skin friction.
With an augmentsin Pr, Le, r, N_b and N_t, the Sherwood number increases.

Conflict of Interest

The authors declare that there is no conflict of interest regarding the publication of this paper.

Acknowledgment

TThis study is supported via funding from Prince Sattam bin Abdulaziz University project number (PSAU/2023/R/1444). The authors are thankful to the Deanship of Scientific Research at University of Bisha for supporting this work through the Fast-Track Research Support Program.

References

[1] K. Hiemenz and D. Grenzschicht, an einem in den gleichformingen flussigkeitsstrom eingetauchten graden kreiszylinder, *Dinglers Polytech J* **326** (1911) 321–324.
[2] S. Pop, I. Pop and T. Grosan, Radiation effects on the flow near the stagnation point of a stretching sheet, *Technische Mechanik-European Journal of Engineering Mechanics* **25**(2) (2005) 100–106.
[3] B. Dutta, P. Roy and A. Gupta, Temperature field in flow over a stretching sheet with uniform heat flux, *International Communications in Heat and Mass Transfer* **12**(1) (1985) 89–94.
[4] C. TC, Stagnation-point flow towards a stretching plate, *Journal of the physical society of Japan* **63**(6) (1994) 2443–2444.
[5] T. R. Mahapatra and A. Gupta, Heat transfer in stagnation-point flow towards a stretching sheet, *Heat and Mass transfer* **38**(6) (2002) 517–521.
[6] R. M. Ramana, K. V. Raju and J. G. Kumar, Multiple slips and heat source effects on mhd stagnation point flow of casson fluid over a stretching sheet in the presence of chemical reaction, *Materials Today: Proceedings* **49** (2022) 2306–2315.
[7] S. Nandi, B. Kumbhakar and S. Sarkar, Mhd stagnation point flow of fe3o4/cu/ag-ch3oh nanofluid along a convectively heated stretching sheet with partial slip and activation energy: Numerical and statistical approach, *International Communications in Heat and Mass Transfer* **130** (2022) p. 105791.
[8] K. K. Asogwa, B. S. Goud, Y. D. Reddy and A. A. Ibe, Suction effect on the dynamics of emhd casson nanofluid over an induced stagnation point flow of stretchable electromagnetic plate with radiation and chemical reaction, *Results in Engineering* **15** (2022) p. 100518.

[9] Y. D. Reddy, B. S. Goud, M. R. Khan, M. A. Elkotb and A. M. Galal, Transport properties of a hydromagnetic radiative stagnation point flow of a nanofluid across a stretching surface *Case Studies in Thermal Engineering* **31**, (Elsevier, 2022), p. 101839.

[10] S. A. Khan, T. Hayat and A. Alsaedi, Cattaneo christov (cc) heat and mass fluxes in stagnation point flow of jeffrey nanoliquids by a stretched surface, *Chinese Journal of Physics* **76** (2022) 205–216.

[11] F. Mabood, A. Abbasi, W. Farooq, Z. Hussain and I. Badruddin, Effects of non-linear radiation and chemical reaction on oldroyd-b nanofluid near oblique stagnation point flow, *Chinese Journal of Physics* **77** (2022) 1197–1208.

[12] A. Mathew, S. Areekara and A. Sabu, Significance of magnetic field and stratification effects on the bioconvective stagnation-point flow of ferro-nanofluid over a rotating stretchable disk: Four-factor response surface methodology, *Journal of the Indian Chemical Society* **99**(8) (2022) p. 100615.

[13] S. Maatoug, S. U. Khan, T. Abbas, E. U. Haq, K. Ghachem, L. Kolsi and A. Abbasi, A lubricated stagnation point flow of nanofluid with heat and mass transfer phenomenon: Significance to hydraulic systems, *Journal of the Indian Chemical Society* **100**(1) (2023) p. 100825.

[14] N. S. Wahid, N. M. Arifin, I. Pop, N. Bachok and M. E. H. Hafidzuddin, Mhd stagnation-point flow of nanofluid due to a shrinking sheet with melting, viscous dissipation and joule heating effects, *Alexandria Engineering Journal* **61**(12) (2022) 12661–12672.

[15] A. Dawar and N. Acharya, Unsteady mixed convective radiative nanofluid flow in the stagnation point region of a revolving sphere considering the influence of nanoparticles diameter and nanolayer, *Journal of the Indian Chemical Society* **99**(10) (2022) p. 100716.

[16] N. C. Roy and I. Pop, Unsteady magnetohydrodynamic stagnation point flow of a nanofluid past a permeable shrinking sheet, *Chinese Journal of Physics* **75** (2022) 109–119.

[17] U. Khan, A. Zaib, S. A. Bakar, N. C. Roy and A. Ishak, Buoyancy effect on the stagnation point flow of a hybrid nanofluid toward a vertical plate in a saturated porous medium, *Case Studies in Thermal Engineering* **27** (2021) p. 101342.

[18] X.-H. Zhang, A. Abidi, A. E.-S. Ahmed, M. R. Khan, M. El-Shorbagy, M. Shutaywi, A. Issakhov and A. M. Galal, *MHD stagnation point flow of nanofluid over a curved stretching/shrinking surface subject to the influence of Joule heating and convective condition* (Elsevier, 2021).

[19] R. Rizwana, A. Hussain and S. Nadeem, Mix convection non-boundary layer flow of unsteady mhd oblique stagnation point flow of nanofluid, *International Communications in Heat and Mass Transfer* **124** (2021) p. 105285.

[20] D. Pal and G. Mandal, Magnetohydrodynamic stagnation-point flow of sisko nanofluid over a stretching sheet with suction, *Propulsion and Power Research* **9**(4) (2020) 408–422.

[21] F. Redouane, W. Jamshed, S. S. U. Devi, B. M. Amine, R. Safdar, K. Al-Farhany, M. R. Eid, K. S. Nisar, A.-H. Abdel-Aty and I. S. Yahia, Influence of entropy on brinkman–forchheimer model of mhd hybrid nanofluid flowing in enclosure containing rotating cylinder and undulating porous stratum, *Scientific Reports* **11** (Dec 2021) p. 24316.

[22] F. Shahzad, W. Jamshed, R. W. Ibrahim, K. Sooppy Nisar, M. A. Qureshi, S. M. Hussain, S. S. P. Mohamed Isa, M. R. Eid, A.-H. Abdel-Aty and I. S. Yahia, Comparative numerical study of thermal features analysis between oldroyd-b copper and molybdenum disulfide nanoparticles in engine-oil-based nanofluids flow, *Coatings* **11**(10) (2021) p. 1196.

[23] S. Choi, D. Singer, H. Wang *et al.*, Developments and applications of non-newtonian flows, *Asme Fed* **66** (1995) 99–105.

[24] J. A. Eastman, S. Choi, S. Li, W. Yu and L. Thompson, Anomalously increased effective thermal conductivities of ethylene glycol-based nanofluids containing copper nanoparticles, *Applied physics letters* **78**(6) (2001) 718–720.

[25] N. Bachok, A. Ishak and I. Pop, Boundary-layer flow of nanofluids over a moving surface in a flowing fluid, *International Journal of Thermal Sciences* **49**(9) (2010) 1663–1668.

[26] P. Priyadharshini and M. V. Archana, Augmentation of magnetohydrodynamic nanofluid flow through a permeable stretching sheet employing machine learning algorithm, *Examples and Counterexamples* **3** (2023) p. 100093.

[27] M. Hussain and M. Sheremet, Convection analysis of the radiative nanofluid flow through porous media over a stretching surface with inclined magnetic field, *International Communications in Heat and Mass Transfer* **140** (2023) p. 106559.

[28] K. Hosseinzadeh, M. Mardani, M. Paikar, A. Hasibi, T. Tavangar, M. Nimafar, D. Ganji and M. B. Shafii, Investigation of second grade viscoelastic non-newtonian nanofluid flow on the curve stretching surface in presence of mhd, *Results in Engineering* **17** (2023) p. 100838.

[29] U. Manzoor, S. M. R. S. Naqvi, T. Muhammad, H. Naeem, H. Waqas and A. M. Galal, Hydro-magnetic impact on the nanofluid flow over stretching/shrinking sheet using keller-box method *International Communications in Heat and Mass Transfer* **135**, (Elsevier, 2022), p. 106114.

[30] S. U. Rehman, A. Mariam, A. Ullah, M. I. Asjad, M. Y. Bajuri, B. A. Pansera and A. Ahmadian, Numerical computation of buoyancy and radiation effects on mhd micropolar nanofluid flow over a stretching/shrinking sheet with heat source, *Case Studies in Thermal Engineering* **25** (2021) p. 100867.

[31] S. Ghasemi and M. Hatami, Solar radiation effects on mhd stagnation point flow and heat transfer of a nanofluid over a stretching sheet, *Case Studies in Thermal Engineering* **25** (2021) p. 100898.

[32] N. A. Zainal, R. Nazar, K. Naganthran and I. Pop, Unsteady emhd stagnation point flow over a stretching/shrinking sheet in a hybrid al2o3-cu/h2o nanofluid *International Communications in Heat and Mass Transfer* **123**, (Elsevier, 2021), p. 105205.

[33] A. A. A. Arani and H. Aberoumand, Stagnation-point flow of ag-cuo/water hybrid nanofluids over a permeable stretching/shrinking sheet with temporal stability analysis, *Powder Technology* **380** (2021) 152–163.

[34] A. B. Jafar, S. Shafie and I. Ullah, Mhd radiative nanofluid flow induced by a nonlinear stretching sheet in a porous medium, *Heliyon* **6**(6) (2020).

[35] P. Patil, M. Kulkarni and P. Hiremath, Effects of surface roughness on mixed convective nanofluid flow past an exponentially stretching permeable surface, *Chinese Journal of Physics* **64** (2020) 203–218.
[36] P. S. Babu, M. V. S. Rao and K. Gangadhar, Boundary layer flow of radioactive non-newtonian nanofluid embedded in a porous medium over a stretched sheet using the spectral relaxation method, *Materials Today: Proceedings* **19** (2019) 2672–2680.
[37] L. A. Lund, Z. Omar and I. Khan, Quadruple solutions of mixed convection flow of magnetohydrodynamic nanofluid over exponentially vertical shrinking and stretching surfaces: Stability analysis, *Computer methods and programs in biomedicine* **182** (2019) p. 105044.
[38] F. Redouane, W. Jamshed, S. S. U. Devi, M. Prakash, N. A. A. M. Nasir, Z. Hammouch, M. R. Eid, K. S. Nisar, A. B. Mahammed, A.-H. Abdel-Aty, I. S. Yahia and E. M. Eed, Heat flow saturate of ag/mgo-water hybrid nanofluid in heated trigonal enclosure with rotate cylindrical cavity by using galerkin finite element, *Scientific Reports* **12** (Feb 2022) p. 2302.
[39] R. M. Muntazir, M. Mushtaq, S. Shahzadi and K. Jabeen, Mhd nanofluid flow around a permeable stretching sheet with thermal radiation and viscous dissipation, *Proceedings of the Institution of Mechanical Engineers, Part C: Journal of Mechanical Engineering Science* **236**(1) (2022) 137–152.
[40] Y. S. Daniel, Z. A. Aziz, Z. Ismail and F. Salah, Thermal radiation on unsteady electrical mhd flow of nanofluid over stretching sheet with chemical reaction, *Journal of King Saud University-Science* **31**(4) (2019) 804–812.
[41] M. Alrehili, Viscoelastic thermal nanofluid flow and heat mass transfer due to a stretching sheet with slip velocity phenomenon and convective heating, *International Journal of Thermofluids* **17** (2023) p. 100281.
[42] T. Muhammad, H. Waqas, U. Farooq and M. Alqarni, Numerical simulation for melting heat transport in nanofluids due to quadratic stretching plate with nonlinear thermal radiation, *Case Studies in Thermal Engineering* **27** (2021) p. 101300.
[43] P. Agrawal, P. K. Dadheech, R. Jat, K. S. Nisar, M. Bohra and S. D. Purohit, Magneto marangoni flow of γ- al2o3 nanofluids with thermal radiation and heat source/sink effects over a stretching surface embedded in porous medium, *Case Studies in Thermal Engineering* **23** (2021) p. 100802.
[44] M. Bhatti, M. Sheikholeslami, A. Shahid, M. Hassan and T. Abbas, Entropy generation on the interaction of nanoparticles over a stretched surface with thermal radiation, *Colloids and Surfaces A: Physicochemical and Engineering Aspects* **570** (2019) 368–376.
[45] S. Mohammadein, K. Raslan, M. Abdel-Wahed and E. M. Abedel-Aal, Kkl-model of mhd cuo-nanofluid flow over a stagnation point stretching sheet with nonlinear thermal radiation and suction/injection, *Results in Physics* **10** (2018) 194–199.
[46] V. Agarwal, B. Singh and K. S. Nisar, Numerical analysis of heat transfer in magnetohydrodynamic micropolar jeffery fluid flow through porous medium over a stretching sheet with thermal radiation, *Journal of Thermal Analysis and Calorimetry* **147**(17) (2022) 9829–9851.
[47] V. Agarwal, B. Singh, A. Kumari, W. Jamshed, K. S. Nisar, A. H. Almaliki and H. Zahran, Steady magnetohydrodynamic micropolar fluid flow and heat and mass transfer in permeable channel with thermal radiation, *Coatings* **12**(1) (2021) p. 11.
[48] F. Shahzad, W. Jamshed, K. S. Nisar, M. M. Khashan and A.-H. Abdel-Aty, Computational analysis of ohmic and viscous dissipation effects on mhd heat transfer flow of cu-pva jeffrey nanofluid through a stretchable surface, *Case Studies in Thermal Engineering* **26** (2021) p. 101148.
[49] A. J. Alqarni, R. E. Abo-Elkhair, E. M. Elsaid, A.-H. Abdel-Aty and M. S. Abdel-wahed, Effect of magnetic force and moderate reynolds number on mhd jeffrey hybrid nanofluid through peristaltic channel: application of cancer treatment, *The European Physical Journal Plus* **138**(2) (2023) p. 137.
[50] Y. Dadhich, R. Jain, A. R. Kaladgi, M. Alwetaishi, A. Afzal and C. A. Saleel, Thermally radiated jeffery fluid flow with nanoparticles over a surface of varying thickness in the influence of heat source, *Case Studies in Thermal Engineering* **28** (2021) p. 101549.
[51] R. S. Saif, T. Muhammad, H. Sadia and R. Ellahi, Hydromagnetic flow of jeffrey nanofluid due to a curved stretching surface, *Physica A: Statistical Mechanics and its Applications* **551** (2020) p. 124060.
[52] F. Shahzad, W. Jamshed, K. S. Nisar, N. A. A. M. Nasir, R. Safdar, A.-H. Abdel-Aty and I. S. Yahia, Thermal analysis for al_2o_3-sodium alginate magnetized jeffrey's nanofluid flow past a stretching sheet embedded in a porous medium, *Scientific Reports* **12**(1) (2022) p. 3287.
[53] S. Rosseland, *Astrophysik: Auf atomtheoretischer grundlage* (Springer, 1931).